Exhibit A

Oncogene (2004) 23, 8292–8300

www.nature.com/onc

Allelic imbalance of *APAF-1* locus at *12q23* is related to progression of colorectal carcinoma

Naoyuki Umetani[1], Akihide Fujimoto[1], Hiroya Takeuchi[1], Masaru Shinozaki[1], Anton J Bilchik[2] and Dave S B Hoon*[,1]

[1]*Department of Molecular Oncology, John Wayne Cancer Institute, Saint Johns Health Science Center, Santa Monica, CA 90404, USA;* [2]*Division of Gastrointestinal Oncology, John Wayne Cancer Institute, Saint Johns Health Science Center, Santa Monica, CA 90404, USA*

***APAF-1* gene, located at chromosome locus *12q23*, is a key factor in the mitochondrial apoptotic pathway downstream of *p53*, and is a potential tumor suppressor gene. We hypothesized that *APAF-1* gene dysfunction due to allelic imbalance (AI) contributes to the development and progression of colorectal carcinoma (CRC). AI at *APAF-1* locus and microsatellite instability (MIN) in CRCs and adenomas were assessed by multiple microsatellite markers. The frequency of AI significantly increased with tumor progression; 0 of 33 (0%) adenomas, 14 of 49 (29%) primary CRCs, and 18 of 34 (53%) liver metastases had AI. A total of 12 metastases were matched with corresponding primary CRCs; in 11 of 12 (92%) pairs, the metastasis had same AI status as the corresponding primary tumor. *APAF-1* mRNA transcription level was significantly decreased with AI in liver metastases ($P=0.009$). Promoter hypermethylation was found in three of 35 (9%) primary CRCs and one of 15 (7%) liver metastases by methylation-specific PCR but was not correlated with AI. MIN was observed in 11 of 49 (23%) primary CRCs and was a favorable prognostic factor. Our results suggest that *APAF-1* gene haploinsufficiency caused by AI increases with tumor progression, and relates to hepatic metastasis.**

Oncogene (2004) **23**, 8292–8300. doi:10.1038/sj.onc.1208022
Published online 20 September 2004

Keywords: allelic imbalance; *APAF-1*; colorectal carcinoma; apoptosis; chromosome *12q23*

Introduction

Sporadic colorectal carcinoma (CRC) arises as a result of a series of somatic mutations, epigenetic inactivation of tumor suppressor genes, and/or activation of oncogenes. Two pathways, the chromosomal instability (CIN) pathway and the microsatellite instability (MIN) pathway, have been proposed and widely accepted (Lengauer *et al.*, 1998). Loss of heterozygosity (LOH) that causes allelic imbalance (AI) and haploinsufficiency is a hallmark of the CIN pathway, whereas MIN characterizes the MIN pathway. In CRC, previous studies have revealed that accumulations of AI at 8p21–pter, 15q11–q21, 17p12–13, and 18q12–21 (*DCC*, *SMAD2*, and *DPC4*/*SMAD4*) were strongly associated with the progression of adenoma to carcinoma (Hermsen *et al.*, 2002). AI of chromosome 18q is an unfavorable prognostic marker in patients with stage II CRC (Jen *et al.*, 1994) and in patients with stage III CRC receiving fluorouracil-based adjuvant chemotherapy (Watanabe *et al.*, 2001), whereas MIN is reportedly a favorable prognostic indicator in patients with CRC (Gryfe *et al.*, 2000; Hemminki *et al.*, 2000).

Epigenetic inactivation by hypermethylation of promoter regions of tumor suppressor genes such as *p16*, *APC*, *VHL*, and *hMLH1* has been found in CRCs (Baylin *et al.*, 1998; Deng *et al.*, 1999; Jones, 1999; Esteller *et al.*, 2000; Robertson and Jones, 2000; Xiong *et al.*, 2001; Herman, 2002). Methylation of cytosines in CpG islands in the promoter region affects promoter activity and can downregulate gene transcription (Jones, 1999). Because the promoter hypermethylation of genes in carcinoma cells is as significant as deletions or mutations (Jones, 1996; Esteller and Herman, 2002; Herman and Baylin, 2003), hypermethylation of key regulatory genes can play a significant role in transformation of colon epithelium as well as tumor progression.

APAF-1, a key factor in the mitochondrial apoptotic pathway downstream of *p53* (Robles *et al.*, 2001), is associated with resistance to apoptosis. Activated *p53* is a transcriptional transactivator of genes that controls the release of cytochrome *c* from mitochondria during apoptosis (Fortin *et al.*, 2001; Moroni *et al.*, 2001; Robles *et al.*, 2001; Mihara *et al.*, 2003). In the presence of cytochrome *c*, *APAF-1* can bind to procaspase 9 and form an apoptosome. Activation of caspase 9 in the apoptosome results in activation of downstream caspases such as 3, 6, and 7 (Li *et al.*, 1997). Consequently, the loss of *APAF-1* gene function leads to defects in the execution of apoptotic programmed cell death and may account for cellular resistance to chemo-, radio-, and

*Correspondence: DSB Hoon, Department of Molecular Oncology, John Wayne Cancer Institute, 2200 Santa Monica Blvd, Santa Monica, CA 90404, USA; E-mail: hoon@jwci.org
Received 20 May 2004; revised 6 July 2004; accepted 6 July 2004; published online 20 September 2004

immunotherapy. *APAF-1* is located at chromosome loci *12q23* (Kim *et al*., 1999), and frequent AI in the *12q22–23* region has been reported in melanomas (Soengas *et al*., 2001; Fujimoto *et al*., 2004), male germ cell tumors (Murty *et al*., 1996), and pancreatic (Kimura *et al*., 1998; Yatsuoka *et al*., 2000), ovarian (Hatta *et al*., 1997) and gastric carcinomas (Schneider *et al*., 2003). In melanomas, AI is associated with a reduction of *APAF-1* mRNA expression levels (Soengas *et al*., 2001; Fujimoto *et al*., 2004), and AI in the *12q22–23* region is related to poor prognosis of patients with American Joint Committee on Cancer (AJCC) stage III/IV melanoma (Fujimoto *et al*., 2004). However, the role of *APAF-1* in CRC has not been studied.

Because *p53* gene alteration is common and its function is impaired in most advanced CRCs, the *p53* pathway involving *APAF-1* should be a key route activating apoptosis. We *hypothesized* that *APAF-1* gene dysfunction contributes to the development and progression of CRC. To examine the role of *APAF-1* loss in the tumorigenesis of CRCs, we assessed AI on the *APAF-1* locus of colorectal adenomas, primary CRCs, and liver metastatic lesions. We also assessed epigenetic inactivation of *APAF-1* by promoter hypermethylation to determine gene transcription silencing. In addition, MIN was determined by the analysis of the PCR products of the microsatellite markers to study the involvement of MIN pathway and its relation with the CIN pathway represented by AI of the *APAF-1* locus.

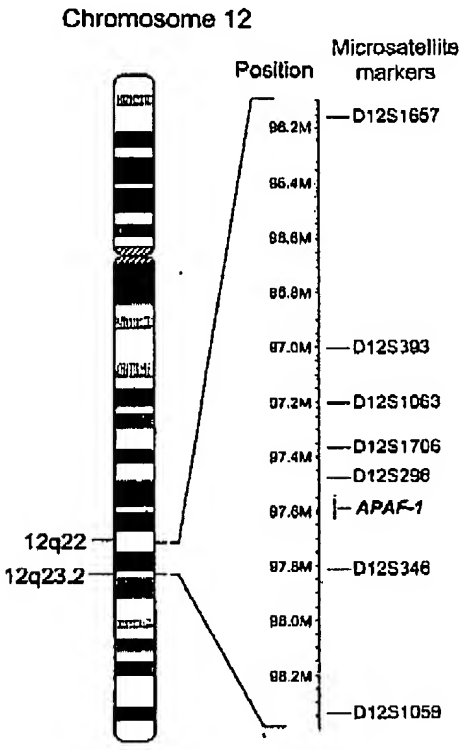

Figure 1 Location of the *APAF-1* gene and microsatellite markers. Location of the *APAF-1* gene and encompassing seven microsatellite markers used for AI assessment. *APAF-1* gene is located at *12q23*, between D12S296 and D12S346. D12S296, located 65 kb centromeric from *APAF-1* gene, is the nearest microsatellite marker

Results

AI at APAF-1 *locus*

To assess the AI status, seven microsatellite markers encompassing the *APAF-1* gene as shown in Figure 1 were assessed for all adenomas, primary CRCs, and liver metastases. AI was indeterminable (noninformative in all microsatellite markers) in three of 119 tumors. One was a liver metastasis showing homozygosity in all microsatellite markers; the other two were liver metastases showing MIN in all heterozygous microsatellite markers. Representative capillary array electrophoresis (CAE) results demonstrating AI in tumors are shown in Figure 2a. In the remaining 116 specimens, which have at least one informative microsatellite marker, none of 33 (0%) adenomas, 14 of 49 (29%) primary CRCs, and 18 of 34 (53%) liver metastases had AI at *APAF-1* locus (Figure 3). The frequency of AI increased significantly as the tumor progressed from adenoma to primary CRC and then to metastasis. The AI frequency was significantly higher in primary CRCs than in adenomas ($P=0.0005$, Fisher's exact test), and was significantly higher in liver metastases than in primary CRCs ($P=0.038$, Fisher's exact test). AI at *APAF-1* locus in liver metastases did not correlate with the size or number of metastasis in the liver (data not shown). Among the seven microsatellite markers, D12S296 was closest to the *APAF-1* gene (65 kb centromeric) and had the highest AI frequency (38%) in primary CRC specimens. As shown in Table 1, no relation was found between AI status and other clinicopathological characteristics (sex, age, tumor site, AJCC TNM scores and stage, histopathological grade, and tumor diameter) in primary CRCs. Among 49 patients with primary CRCs, no correlation with AI status and survival was found by univariate Cox's proportional hazard model (Table 2).

Methylation status of APAF-1 *promoter region*

Methylation status of *APAF-1* promoter region was assessed in 35 primary CRCs (seven AI (+) and 28 AI (−) tumors) and 15 liver metastases (six AI (+) and nine AI (−) tumors). Methylation status was determined by methylated-specific and unmethylated-specific peaks by methylation-specific PCR (MSP) (Figure 4). DNA from normal peripheral blood lymphocytes (PBLs) showed only an unmethylated-specific peak (Figure 4a), whereas *Sss*I methylase-treated (forced hypermethylation) DNA showed only a methylated-specific peak (Figure 4b). Hypermethylation was found in three of 35 (9%) primary CRCs and one of 15 (7%) liver metastases by MSP. There was no correlation between methylation status and AI status at *APAF-1* locus. All AI (+) specimens were unmethylated.

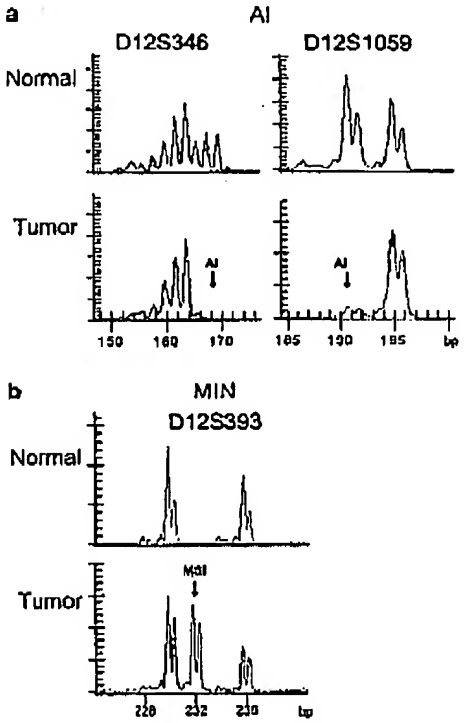

Figure 2 Representative CAE results of AI and MIN. (a) Representative CAE results demonstrating AI in tumors. Peaks with reduced fluorescent intensity of PCR amplicon of microsatellite markers are indicated by arrows. (b) Representative CAE result demonstrating MIN in a tumor. A peak representing aberrant PCR amplicon size of a microsatellite marker is indicated by an arrow. In both panels, the vertical axis represents the fluorescent intensity indicating the amount of PCR amplicon and the horizontal axis represents the PCR amplicon size

APAF-1 *AI and mRNA expression level*

To evaluate the effect of AI on mRNA transcription level, we assessed the mRNA level of representative liver metastatic specimens with known AI status. Tumor mRNA was extracted from precisely dissected tumor cells using the PixCell II Laser Capture Microdissection (LCM) System (Arcturus Engineering, Mountain View, CA, USA), avoiding contamination of nontumor cells. Absolute copy numbers of *APAF-1* and *GAPDH* in 250 ng of total RNA were quantified by quantitative real-time reverse-transcriptase PCR (qRT–PCR). To minimize the influence of formalin fixation and degradation of the mRNA, the relative copy number of *APAF-1* against the *GAPDH* house-keeping gene was used instead of the absolute copy number of *APAF-1*. Relative copy numbers of *APAF-1* of the five AI (+) liver metastases and five AI (−) liver metastases were $5.9 \pm 1.1 \times 10^{-2}$ and $10.7 \pm 0.9 \times 10^{-2}$ (mean ± s.e.m.), respectively. The transcription level of mRNA was significantly lower in AI (+) tumors than in AI (−) tumors ($P = 0.009$, Wilcoxon's rank-sum test) (Figure 5). The average mRNA transcription level of AI (−) tumors was approximately twice that of AI (+) tumors, and it was consistent with the expected haploinsufficiency caused by the AI of the tumors.

Concordance of AI between a liver metastasis and its primary CRC

A total of 12 liver metastases [three AI (−) and nine AI (+)] were matched with their primary CRCs to study the concordance of AI status in the development of liver metastasis. The metastasis and its primary CRC had the same AI status in 11 of 12 (92%) pairs: three AI (−) and eight AI (+). In the remaining pair, the primary CRC was AI (−) but the metastasis was AI (+).

Microsatellite instability

MIN was determined by the analysis of PCR products of the AI study. Representative CAE result demonstrating MIN in a tumor is shown in Figure 2b. Three of 33 (9%) adenomas, 11 of 49 (23%) primary CRCs, and seven of 37 (19%) liver metastases showed MIN in one or more microsatellite marker analyses. There was no correlation between MIN status and AI status of *APAF-1* locus. Among the 49 patients with primary CRCs, those with MIN (+) primary CRC had significantly better prognosis by univariate Cox's proportional hazard model ($P = 0.003$) (Table 2) and by multivariate Cox's proportional hazard model ($P = 0.0001$) with covariates of AJCC T, N, and M scores and histopathological grade (Table 3).

Discussion

In the model of genetic alteration in colorectal carcinogenesis (Vogelstein *et al*., 1988), K-*ras* mutation and AI at the *APC* gene locus are early genetic changes that occur in adenomas, whereas AI of 18q (*DCC*, *SMAD2*, and *DPC4/SMAD4*) and 17q (*p53*) are late significant events. Invasive cancer cells require a mechanism for avoiding apoptosis to survive. Inactivation of *p53* gene, which is a component of an apoptotic pathway, is common in most advanced CRCs, but infrequent in colorectal adenomas (Hao *et al*., 2002). Therefore, it is suggested that the *p53* apoptotic pathway is inactivated when tumor cells transform from adenoma into carcinoma. Considering that *APAF-1* gene is a key factor in the mitochondrial apoptotic pathway downstream of *p53* (Robles *et al*., 2001) and necessary for the later activation phase of apoptosis, inactivation of *APAF-1* gene may also be important for colorectal carcinogenesis. Tumor cells with *APAF-1* downregulation are expected to be advantageous for survival by escaping from extracellular apoptotic signals such as tumor necrosis factor (TNF) and TNF-related apoptosis-inducing ligand (TRAIL). Therefore, we hypothesized that *APAF-1* inactivation or downregulation caused by AI at *APAF-1* locus might affect tumor cell resistance from apoptotic signals and thereby facilitate progression of CRC. To know the frequency of occurrence of AI at *APAF-1* locus in the carcinogenic

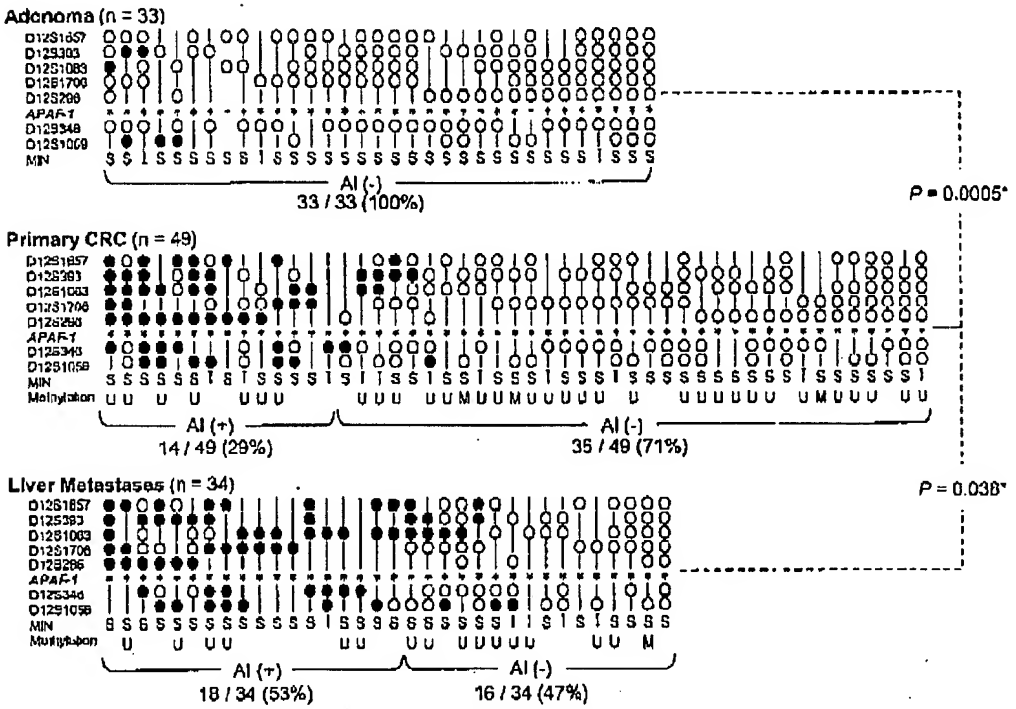

Figure 3 Details of the analysis of AI status, methylation status, and MIN in tissues. Analysis of AI status, methylation status at promoter region, and MIN in tissues. Closed circles (•) represent AI (+), open circles (O) represent AI (−), and vertical bars (|) indicate noninformative. Asterisks (*) show the locus of *APAF-1* gene. The AI frequency was significantly higher in primary CRCs than in adenomas ($P = 0.0005$, Fisher's exact test), and was significantly higher in liver metastases than primary CRCs ($P = 0.038$, Fisher's exact test). 'M' represents hypermethylated and 'U' unmethylated CpG islands in the promoter region. 'I' represents MIN (+) tumors (instable in one or more microsatellite markers) and 'S' represents MIN (−) tumors (stable in all microsatellite markers)

pathway, we studied AI in adenoma, primary CRC, and liver metastasis, representing each progressive stage of colorectal carcinogenesis.

In this study, AI at *APAF-1* locus was found in primary or metastatic CRCs but not in adenomas. Therefore, this genetic alteration may potentially be important in CRC development, like the other genetic alterations found in the later stage of colorectal carcinogenesis, such as *p53* gene inactivation or deletion of 18q. In addition, the significantly higher frequency of AI in liver metastases than in primary CRCs suggests that AI at *APAF-1* gene locus may facilitate liver metastasis. The high frequency of AI at *APAF-1* locus in liver metastases supports a correlation between the ability of cancer cells to escape apoptotic signals and its likelihood of metastasizing to distant sites such as the liver. Therefore, AI of *APAF-1* gene expression might be expected to have an adverse effect on prognosis. However, despite a trend for better prognosis in patients with AI (−) primary tumors, there was no significant correlation between AI status of primary CRC and overall survival. This may be due to effective therapeutic interventions. Further investigation with a larger series of patients from randomized controlled study will be required to determine the prognostic significance of AI at *APAF-1* in primary CRC.

In this study, there was no significant correlation between AI at *APAF-1* locus in primary CRC and AJCC N and M scores. However, the frequency of AI in the liver metastases was higher than that in the primary CRCs. We speculate that cancer cells in a primary lesion transformed to AI (+) at *APAF-1* locus obtain potential of escaping from apoptosis. This event combined with metastasis to the liver allows a greater probability of survival of the spreading cancer cells at a distant site. The reason as to why the frequencies of AI (+) in M1 and N1 or N2 tumors are not significantly higher may be related to the heterogeneity of the tumor cells in the primary CRCs. In general, detection of AI (+) cells using microsatellite markers can be easily affected by the contamination of AI (−) cells. Tumors having <50% AI (+) cancer cells would be determined as AI (−) with our definition. Therefore, the tumors harboring AI (+) cells in part, which would have been determined as AI (−) in our study, could have metastatic potential.

In the concordance analysis with 12 pairs of primary CRCs and liver metastases, there was only one pair in which AI status changed (the primary lesion was AI (−) but the metastasis was AI (+)), while the other pairs maintained AI status during the development of metastasis. Because apoptosis-resistant clones are more

Table 1 AI at *APAF-1* locus and clinicopathological characteristics for 49 patients with AJCC stage I–IV primary CRC

Variable	*No. of patients (% of total)*		*P-value*
	AI (+)	*AI (−)*	
Total no. of patients	14 (29)	35 (71)	
Sex			0.75[a]
Male	5 (24)	16 (76)	
Female	9 (32)	19 (68)	
Age (years)			
Median	63.5	72	0.43[b]
Range	39–93	40–94	
Tumor site			0.53[a]
Right colon	6 (23)	20 (77)	
Left colon/rectum	8 (35)	15 (65)	
AJCC primary tumor (T)			0.32[c]
T1	1 (17)	5 (83)	
T2	3 (60)	2 (40)	
T3	9 (29)	22 (71)	
T4	1 (14)	6 (86)	
AJCC regional lymph nodes (N)			0.33[c]
N0	7 (26)	20 (74)	
N1	3 (21)	11 (79)	
N2	4 (50)	4 (50)	
AJCC distant metastasis (M)			0.75[a]
M0	8 (27)	22 (73)	
M1	6 (32)	13 (68)	
AJCC stage			0.97[c]
I	3 (30)	7 (70)	
II	3 (25)	9 (75)	
III	2 (25)	6 (75)	
IV	6 (32)	13 (68)	
Histopathological grade			0.50[a]
Well/moderate	11 (32)	23 (68)	
Poor/undifferentiated	3 (20)	12 (80)	
Tumor diameter (mm)			
Median	42.5	47	0.23[b]
Range	18–85	9–100	

[a]Fisher's exact test. [b]Wilcoxon's rank-sum test. [c]χ^2 test

Table 2 Univariate analysis of overall survival of 49 patients with AJCC stage I–IV primary CRC

Variable	*Relative risk (95% CI)*	*P-value*
Age	1.01 (0.97, 1.04)	0.75
Tumor site		0.92
(left/rectum)	0.98 (0.64, 1.49)	
Tumor diameter	1.03 (1.01, 1.04)	0.002
AJCC primary tumor (T)		0.002
(T3–T1/T2)	7.37 (1.49, 133.2)	
(T4–T3)	2.74 (0.94, 7.12)	
AJCC regional lymph nodes (N)		0.004
(N1–N0)	3.23 (1.15, 9.23)	
(N2–N1)	1.81(0.62, 5.20)	
AJCC distant metastasis (M)		<0.0001
(M1–M0)	14.3 (5.36, 45.7)	
AJCC stage		<0.0001
(II–I)	0.86 (0.03, 21.6)	
(III–II)	4.81 (0.61, 97.2)	
(IV–III)	6.06 (1.95, 26.7)	
Histopathological grade		0.016
(poor/undifferentiated)	1.70 (1.11, 2.61)	
APAF-1 AI status		0.71
(AI (+))	1.09 (0.67, 1.68)	
APAF-1 methylation status		0.50
(methylated)	1.32 (0.52, 2.49)	
MSI		0.003
(MSI (−))	2.96 (1.35, 12.5)	

[a]By Cox's proportional hazard model

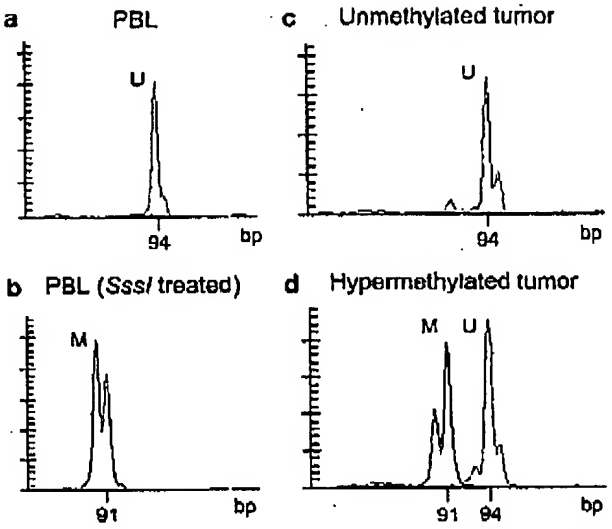

Figure 4 Representative CAE results of MSP. The vertical axis represents the fluorescent intensity indicating the amount of PCR amplicon. (a) DNA from normal PBL used as a negative control. Unmethylated-specific peak at 94 bp indicated as 'U' is observed. (b) *Sss*I methylase-treated (forced hypermethylation) DNA obtained from PBL used as a positive control. Methylated-specific peak at 91 bp indicated as 'M' is observed. (c) Example of unmethylated tumor. Only an unmethylated-specific peak is observed. (d) Example of a hypermethylated tumor. Both methylated- and unmethylated-specific peaks are observed. Tumor specimens showing methylated-specific peak were determined as hypermethylated

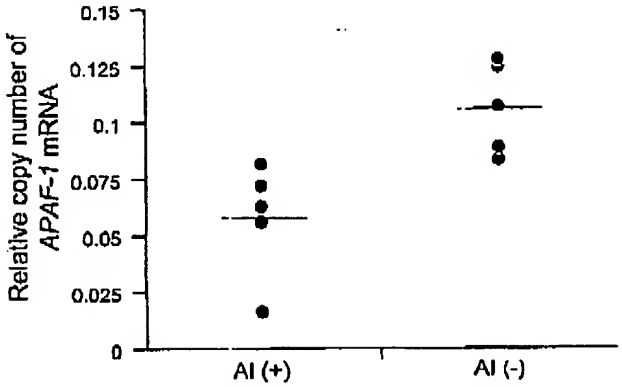

Figure 5 *APAF-1* mRNA expression in AI (+) and AI (−) liver metastases. Relative copy numbers of *APAF-1* mRNA against *GAPDH* mRNA in five AI (+) liver metastases and five AI (−) liver metastases were $5.9 \pm 1.1 \times 10^{-2}$ and $10.7 \pm 0.9 \times 10^{-2}$ (mean ± s.e.m.), respectively. Relative copy number was significantly lower in AI (+) tumors than in AI (−) tumors ($P = 0.009$, Wilcoxon's rank-sum test). The horizontal bars indicate the mean value of each group

likely to survive during the process of metastasis to the liver, clones with haploinsufficiency of *APAF-1* caused by AI should become dominant in the metastatic lesions. AI (+) primary CRCs were suggested to have higher ability to metastasize than AI (−) primary CRCs

Table 3 Multivariate analysis of overall survival of 49 patients with AJCC stage I–IV primary CRC

Covariate	*Relative risk (95% CI)*	*P-value*[a]
AJCC primary tumor (T)		0.16
(T3–T1/T2)	1.74 (0.25, 34.6)	
(T4–T3)	0.29 (0.07, 1.09)	
AJCC regional lymph nodes (N)		0.0089
(N1–N0)	5.29 (1.54, 19.6)	
(N2–N1)	1.30 (0.41, 4.04)	
AJCC distant metastasis (M)		<0.0001
(M1–M0)	10.6 (3.52, 40.5)	
Histopathological grade		0.026
(poor/undifferentiated)	1.87 (1.08, 3.33)	
MSI		0.0001
(MSI (−))	6.24 (2.23, 30.0)	

[a]By Cox's proportional hazard model

because majority of the primary CRCs had same AI status of their metastases.

The relations between AI at *APAF-1* locus and mRNA transcription level in liver metastases were assessed to ascertain the correlation between AI status and mRNA expression level of *APAF-1* gene. Because liver metastases have fewer nontumor cells such as stromal cells compared to primary CRCs, they are more suitable for mRNA expression study, which is sensitive to contamination by nontumor cells. qRT–PCR results revealed that AI (+) tumors had significantly lower expression level of mRNA than AI (−) tumors, in accordance with the results of our previous study in melanoma (Fujimoto *et al*., 2004). The relative mRNA level was reduced to 45% in AI (+) tumors; this reduction can be explained as a haploinsufficiency caused by deletion of one allele. Extracellular apoptotic signals on tumor cells may induce expression of *APAF-1* gene, but the transcription rate would be limited by the reduction of the allele number.

Methylation status of *APAF-1* gene was also studied. Hypermethylation of promoter region of a gene is an important mechanism of epigenetic gene silencing. Because many tumor-related genes have been reported to be inactivated by promoter hypermethylation along with AI, we assessed the methylation status of *APAF-1* promoter region. Hypermethylation of *APAF-1* occurred in low frequency and was absent in AI (+) tumors. This suggests that hypermethylation is not a major factor silencing *APAF-1* expression in CRC.

After the initial publication of AI at *APAF-1* gene in melanomas by Soengas *et al*. (2001), the *APAF-1* gene locus was reassessed. The current information in the National Center for Biotechnology Information (NCBI) database indicates that the *APAF-1* gene is located more distal (>0.3 Mb) from the chromosome 12q centromere, and this location change may significantly affect the result of AI study. Therefore, we studied AI status by seven microsatellite markers that encompassed not only the current *APAF-1* locus between D12S296 and D12S346 but also the locus between D12S1657 and D12S393, which previously had been considered the locus of *APAF-1*. In the present study, the frequency of AI between D12S1657 and D12S393 would be evaluated as 0–6, 18–31, and 56–62% in adenomas, primary CRCs, and liver metastases, respectively. The high frequency of AI at this locus in liver metastases suggests the presence of other tumor suppressor genes or tumor-related genes near the microsatellite markers D12S1657 and D12S393. Currently, there is no known or definite candidate tumor suppressor gene identified in the vicinity of this locus.

The MIN pathway is as important as the CIN pathway in colorectal carcinogenesis (Lengauer *et al*., 1998), and MIN status can be evaluated by using microsatellite markers located throughout the genome. We evaluated the MIN status from the CAE results of microsatellite markers used for *APAF-1* gene AI study. MIN has been reported in approximately 13–16% of sporadic CRCs and in virtually all CRCs arising in patients with hereditary nonpolyposis colorectal cancer (HNPCC) (Aaltonen *et al*., 1993; Thibodeau *et al*., 1993; Herman *et al*., 1998). In this study, we found a similar frequency of MIN (+) CRCs, and MIN was independent of AI at *APAF-1*. Consistent with the previous report that associated MIN (+) phenotype with favorable prognosis (Gryfe *et al*., 2000; Hemminki *et al*., 2000), our results showed that patients with MIN (+) primary CRCs had favorable prognosis by univariate and multivariate survival analyses and that MIN status of primary CRC was an independent prognostic factor.

In conclusion, AI of *APAF-1* locus at *12q23* was not found in colorectal adenomas but was frequent in primary CRCs and liver metastases of CRC. The frequency of AI was significantly higher in liver metastases, and expression level of *APAF-1* mRNA was correlated with AI status. The haploinsufficiency caused by AI of *APAF-1* gene may favor the development of clinically significant CRC metastases.

Materials and methods

Tissue samples and clinicopathological information

We analysed AI status of 119 neoplastic colorectal tumors (33 adenomas, 49 primary CRCs, and 37 liver metastases) from 89 patients selected by the database coordinator based on those patients who underwent colectomy, proctectomy, or endoscopic treatment between 1995 and 2001 at Saint John's Health Center, Santa Monica. The primary CRCs were collected from AJCC stage I–IV carcinomas. The liver metastases were surgically resected synchronous or metachronous metastases of CRC. For *APAF-1* mRNA expression analysis, 10 specimens of liver metastases were studied. All specimens were formalin-fixed, paraffin-embedded archival tissues (PEAT) obtained from the pathology department. Tumor tissues were reviewed by the pathologist to confirm histopathologic status. All patients in this study consented and the study was according to the guidelines set forth by JWCI Institutional Review Board (IRB) committee. Tumors were classified and staged according to the revised guidelines set by the AJCC. Clinicopathological data from the tumor registry were obtained after IRB approval for all patients.

To study the concordance of AI status during development of liver metastasis, AI status was assessed in 12 liver metastases and their corresponding primary CRCs.

DNA extraction and sodium bisulfite modification of DNA

Several 5-μm sections were cut with a microtome from PEAT under sterile conditions as previously described (Shinozaki *et al.*, 2004). One section for each tumor was stained with hematoxylin after deparaffinization and the neoplastic lesions were precisely dissected using LCM as previously described (Hoon *et al.*, 2002). Dissected tissues were digested with 50 μl of proteinase K containing lysis buffer at 50°C for 5 h, followed by heat deactivation of proteinase K at 95°C for 10 min. Lysate was directly used as a template for PCR as previously described (Nakayama *et al.*, 2001; Hoon *et al.*, 2002). Control (non-neoplastic) DNA for each tumor was obtained from its tumor-adjacent normal tissue, that is, normal mucosa for primary CRCs or adenomas, and normal liver tissue for liver metastases of same sections of the tumors. Sodium bisulfite modification was applied on extracted genomic DNA of tissue specimens for MSP as previously described (Spugnardi *et al.*, 2003).

Microsatellite analysis

AI was assessed by seven microsatellite markers (D12S1657, D12S393, D12S1063, D12S1706, D12S296, D12S346, and D12S1059) encompassing the *APAF-1* gene locus at *12q23* (Figure 1). The primer sets were as follows: D12S1657 forward, 5′-TCCTAAAGATGGTGTGCAT-3′; reverse, 5′-AAGTTCCAATGTTAGTGAACC-3′; D12S393 forward, 5′-ATTAATGCCAGGACATTAAACG-3′; reverse, 5′-CCTCACACAATGTTGTAAGGG-3′; D12S1063 forward, 5′-ACACAACGATGAAATTGCCT-3′; reverse, 5′-TGGATGAGCCAATTCCTTAA-3′; D12S1706 forward, 5′-CCTATGATTTCCCATCAAGTTT-3′; reverse, 5′-ATTATTAGGAGAGCCCTGGG-3′; D12S296 forward, 5′-GGGAACAAGAGCAAAACTTC-3′; reverse, 5′-TTCAGAACCCATGGACATGG-3′; D12S346 forward, 5′-TGCCCACCTGCCTGTAAC-3′; reverse, 5′-AATGGAGGGTAAATGCCCG-3′; D12S1059 forward, 5′-TGATCCTTTGAGACATTGTACTG-3′; reverse, 5′-CCAGCTTACCAACTGCAGAT-3′. Forward primers were labeled with WellRED dye-labeled phosphoramidites (Beckman Coulter Inc., Fullerton, CA, USA). The PCR amplification was performed in a 10-μl reaction volume with 1 μl template for 40 cycles of 30 s at 94°C, 30 s at 55°C, and 30 s at 72°C, followed by a 7-min final extension at 72°C. PCR product separation was performed using CAE by CEQ 8000XL (Beckman Coulter Inc.). Peak fluorescent intensity indicating the amount of PCR amplicon and the PCR amplicon size were calculated by software for fragment analysis system (Beckman Coulter Inc.). For each microsatellite marker, 50% or more reduction of fluorescent intensity of one allele for tumor DNA as compared to the corresponding control DNA was defined as AI (Figure 2a). The CAE result at each microsatellite marker showing homozygosity in control DNA or MIN in tumor DNA was defined as noninformative. The AI status of the *APAF-1* gene locus of the tumors was determined according to the nearest informative marker. Specimens with no informative markers were indeterminable of AI status and were excluded from AI analysis. MIN was determined by the change of repeating motifs in the microsatellite markers within the tumor when compared to normal tissue as defined previously (Boland *et al.*, 1998). Tumors having instability in one or more microsatellite markers were defined as MIN (+), and tumors stable in all microsatellite markers were defined as MIN (−). A representative CAE result demonstrating MIN in a tumor is shown in Figure 2b.

RNA extraction and analysis of mRNA expression level

For mRNA expression analysis, total RNA was extracted from 10 specimens of metastases. A total of 1–3 5-μm sections of each specimen were stained with methyl green after deparaffinization, and the tumor cells were precisely microdissected using LCM following the manufacturer's protocol of the Paraffin Block RNA Isolation Kit (Ambion, Austin, TX, USA) with modifications (Takeuchi *et al.*, 2004). Quality and quantity of extracted total RNA were measured by UV absorption spectrophotometry to ensure that it was suitable for the assay.

After extraction of total RNA, reverse-transcriptase reactions were performed on 1.0 μg of total RNA using Moloney murine leukemia virus reverse-transcriptase (Promega, Madison, WI, USA) with the mixture of oligo-dT and random hexamers as the primers, as previously described (Takeuchi *et al.*, 2004). qRT–PCR assay was performed on the iCycler iQ Real-Time thermocycler detection system (Bio-Rad Laboratories, Hercules, CA, USA) (Takeuchi *et al.*, 2004). For each PCR, the reaction mixture consisted of cDNA template synthesized from 250 ng of total RNA, 1 μM of forward primer (5′-ACATTTCTCACGATGCTACC-3′) and reverse primer (5′-CAATTCATGAACTGGCAA-3′), and 0.3 μM of fluorescence resonance energy transfer probe (5′-FAM-TGCTGACAAGACTGCAAAGATCTG-BHQ-1-3′). PCR amplification was performed in a 20-μl reaction volume for 45 cycles of 60 s at 94°C, 60 s at 55°C, and 60 s at 72°C. The standard curve was established for quantifying mRNA copy numbers by using nine known copy numbers of serially diluted (10^6–10^0 copies) plasmids containing *APAF-1* cDNA sequence. Reaction without templates was performed as a negative control in each study. PCR products were electrophoresed on 2% agarose gels to confirm correct product size and absence of nonspecific bands. The mRNA expression level of the housekeeping gene *GAPDH* was measured by qRT–PCR as an internal reference with a standard curve to determine the integrity and quality of template RNA for all specimens. The ratio of *APAF-1* and *GAPDH* expression level was calculated as (absolute copy number of *APAF-1*)/(absolute copy number of *GAPDH*) as previously described (Takeuchi *et al.*, 2004).

Detection of promoter hypermethylation

The methylation status of *APAF-1* promoter region was assessed in a subset of specimens from primary tumors and hepatic metastases. The assay involved sodium bisulfite modification followed by MSP to determine the methylation status as previously described (Spugnardi *et al.*, 2003). *Sss*I methylase-treated and -untreated normal DNA obtained from PBL of a healthy donor was used as a positive and a negative control, respectively (Renbaum *et al.*, 1990). Primers used for MSP were as follows: methylated-specific forward, 5′-GTCGTTGTTCGAGTTCGGTA-3′; reverse, 5′-GCGTAAAAATACCCGCCTAC-3′; unmethylated-specific forward, 5′-GGGTGTGTTGTTGTTGTTTGA-3′; reverse, 5′-AAATACCCACCTACCCCACA-3′. Each forward primer contained three CpG sites and each reverse primer contained two CpG sites within the annealing sequence. Forward primers were labeled with WellRED dye-labeled phosphoramidites (Beckman Coulter Inc.). The PCR amplification was performed in a 10-μl reaction volume with 1 μl template for 40 cycles of 30 s at

94°C, 30 s at 55°C, and 30 s at 72°C, followed by a 7-min final extension at 72°C. Detection of PCR products was analysed by CAE using CEQ 8000XL (Beckman Coulter Inc.).

Statistical analysis

The relation between *APAF-1* AI status and tumor classification (adenomas, primary CRCs, liver metastases) was assessed using Fisher's exact test. The relation between *APAF-1* AI status and other clinicopathological or genetic characteristics was assessed using Fisher's exact test, χ^2 test, or Wilcoxon's rank-sum test. For survival analysis, Cox's proportional hazard model was used for univariate and multivariate analyses of clinicopathological or genetic characteristics. Variables suggested by the univariate analyses ($P<0.10$) were entered into the multivariate analysis. For comparison of mRNA expression level, Wilcoxon's rank-sum test was used. The statistical package SAS JMP ver. 5.0.1 (SAS Institute Inc., Cary, NC, USA) was used to conduct statistical analyses. A P-value <0.05 (two-tailed) was considered as significant.

Acknowledgements
This study was supported in part by funding from the Rod Fasone Memorial Cancer Fund (Indianapolis, IN), PO CA 29605 from the National Cancer Institute, NIH, and the Roy E Coates Foundation Laboratory.

References

Aaltonen LA, Peltomaki P, Leach FS, Sistonen P, Pylkkanen L, Mecklin JP, Jarvinen H, Powell SM, Jen J, Hamilton SR, de la Chapelle A and Vogelstein B. (1993). *Science*, **260**, 812–816.
Baylin SB, Herman JG, Graff JR, Vertino PM and Issa JP. (1998). *Adv. Cancer Res.*, **72**, 141–196.
Boland CR, Thibodeau SN, Hamilton SR, Sidransky D, Eshleman JR, Burt RW, Meltzer SJ, Rodriguez-Bigas MA, Fodde R, Ranzani GN and Srivastava S. (1998). *Cancer Res.*, **58**, 5248–5257.
Deng G, Chen A, Hong J, Chae HS and Kim YS. (1999). *Cancer Res.*, **59**, 2029–2033.
Esteller M and Herman JG. (2002). *J. Pathol.*, **196**, 1–7.
Esteller M, Sparks A, Toyota M, Sanchez-Cespedes M, Capella G, Peinado MA, Gonzalez S, Tarafa G, Sidransky D, Meltzer SJ, Baylin SB and Herman JG. (2000). *Cancer Res.*, **60**, 4366–4371.
Fortin A, Cregan SP, MacLaurin JG, Kushwaha N, Hickman ES, Thompson CS, Hakim A, Albert PR, Cecconi F, Helin K, Park DS and Slack RS. (2001). *J. Cell Biol.*, **155**, 207–216.
Fujimoto A, Takeuchi H, Taback B, Hsueh EC, Elashoff D, Morton DL and Hoon DS. (2004). *Cancer Res.*, **64**, 2245–2250.
Gryfe R, Kim H, Hsieh ET, Aronson MD, Holowaty EJ, Bull SB, Redston M and Gallinger S. (2000). *N. Engl. J. Med.*, **342**, 69–77.
Hao XP, Frayling IM, Sgouros JG, Du MQ, Willcocks TC, Talbot IC and Tomlinson IP. (2002). *Gut*, **50**, 834–839.
Hatta Y, Takeuchi S, Yokota J and Koeffler HP. (1997). *Br. J. Cancer*, **75**, 1256–1262.
Hemminki A, Mecklin JP, Jarvinen H, Aaltonen LA and Joensuu H. (2000). *Gastroenterology*, **119**, 921–928.
Herman JG. (2002). *Gastroenterol. Clin. N. Am.*, **31**, 945–958.
Herman JG and Baylin SB. (2003). *N. Engl. J. Med.*, **349**, 2042–2054.
Herman JG, Umar A, Polyak K, Graff JR, Ahuja N, Issa JP, Markowitz S, Willson JK, Hamilton SR, Kinzler KW, Kane MF, Kolodner RD, Vogelstein B, Kunkel TA and Baylin SB. (1998). *Proc. Natl. Acad. Sci. USA*, **95**, 6870–6875.
Hermsen M, Postma C, Baak J, Weiss M, Rapallo A, Sciutto A, Roemen G, Arends JW, Williams R, Giaretti W, De Goeij A and Meijer G. (2002). *Gastroenterology*, **123**, 1109–1119.
Hoon DS, Fujimoto A, Shu S and Taback B. (2002). *Methods Enzymol.*, **356**, 302–309.
Jen J, Kim H, Piantadosi S, Liu ZF, Levitt RC, Sistonen P, Kinzler KW, Vogelstein B and Hamilton SR. (1994). *N. Engl. J. Med.*, **331**, 213–221.
Jones PA. (1996). *Cancer Res.*, **56**, 2463–2467.
Jones PA. (1999). *Trends Genet.*, **15**, 34–37.
Kim H, Jung YK, Kwon YK and Park SH. (1999). *Cytogenet. Cell Genet.*, **87**, 252–253.
Kimura M, Furukawa T, Abe T, Yatsuoka T, Youssef EM, Yokoyama T, Ouyang H, Ohnishi Y, Sunamura M, Kobari M, Matsuno S and Horii A. (1998). *Cancer Res.*, **58**, 2456–2460.
Lengauer C, Kinzler KW and Vogelstein B. (1998). *Nature*, **396**, 643–649.
Li P, Nijhawan D, Budihardjo I, Srinivasula SM, Ahmad M, Alnemri ES and Wang X. (1997). *Cell*, **91**, 479–489.
Mihara M, Erster S, Zaika A, Petrenko O, Chittenden T, Pancoska P and Moll UM. (2003). *Mol. Cell*, **11**, 577–590.
Moroni MC, Hickman ES, Denchi EL, Caprara G, Colli E, Cecconi F, Muller H and Helin K. (2001). *Nat. Cell Biol.*, **3**, 552–558.
Murty VV, Renault B, Falk CT, Bosl GJ, Kucherlapati R and Chaganti RS. (1996). *Genomics*, **35**, 562–570.
Nakayama T, Taback B, Turner R, Morton DL and Hoon DS. (2001). *Am. J. Pathol.*, **158**, 1371–1378.
Renbaum P, Abrahamove D, Fainsod A, Wilson GG, Rottem S and Razin A. (1990). *Nucleic Acids Res.*, **18**, 1145–1152.
Robertson KD and Jones PA. (2000). *Carcinogenesis*, **21**, 461–467.
Robles AI, Bemmels NA, Foraker AB and Harris CC. (2001). *Cancer Res.*, **61**, 6660–6664.
Schneider BG, Rha SY, Chung HC, Bravo JC, Mera R, Torres JC, Plaisance Jr KT, Schlegel R, McBride CM, Reveles XT and Leach RJ. (2003). *Mol. Pathol.*, **56**, 141–149.
Shinozaki M, Fujimoto A, Morton DL and Hoon DS. (2004). *Clin. Cancer Res.*, **10**, 1753–1757.
Soengas MS, Capodieci P, Polsky D, Mora J, Esteller M, Opitz-Araya X, McCombie R, Herman JG, Gerald WL, Lazebnik YA, Cordon-Cardo C and Lowe SW. (2001). *Nature*, **409**, 207–211.
Spugnardi M, Tommasi S, Dammann R, Pfeifer GP and Hoon DS. (2003). *Cancer Res.*, **63**, 1639–1643.
Takeuchi H, Morton DL, Kuo C, Turner RR, Elashoff D, Elashoff R, Taback B, Fujimoto A and Hoon DS. (2004). *J. Clin. Oncol.*, **22**, 2671–2680.
Thibodeau SN, Bren G and Schaid D. (1993). *Science*, **260**, 816–819.

Vogelstein B, Fearon ER, Hamilton SR, Kern SE, Preisinger AC, Leppert M, Nakamura Y, White R, Smits AM and Bos JL. (1988). *N. Engl. J. Med.*, **319**, 525–532.

Watanabe T, Wu TT, Catalano PJ, Ueki T, Satriano R, Haller DG, Benson III AB and Hamilton SR. (2001). *N. Engl. J. Med.*, **344**, 1196–1206.

Xiong Z, Wu AH, Bender CM, Tsao JL, Blake C, Shibata D, Jones PA, Yu MC, Ross RK and Laird PW. (2001). *Cancer Epidemiol. Biomarkers Prev.*, **10**, 799–803.

Yatsuoka T, Sunamura M, Furukawa T, Fukushige S, Yokoyama T, Inoue H, Shibuya K, Takedu K, Matsuno S and Horii A. (2000). *Am. J. Gastroenterol.*, **95**, 2080–2085.